García-Hernando, N., de Vega, M. & Venegas, M. (2019). Experimental characterisation of a novel adiabatic membrane-based micro-absorber using H2O-LiBr. *International Journal of Heat and Mass Transfer*, vol. 129, pp. 1136–1143.

DOI: 10.1016/j.ijheatmasstransfer.2018.10.046

Declarations of interest: none

Experimental characterisation of a novel adiabatic membrane-based micro-absorber using H_2O-LiBr

N. García-Hernando [a], M. de Vega [a], M. Venegas [a,b*]

[a] ISE Research Group, Department of Thermal and Fluids Engineering, Universidad Carlos III de Madrid, Avda. Universidad 30, 28911 Leganés, Madrid, Spain
[b] GTADS Research Group, Department of Thermal and Fluids Engineering, Universidad Carlos III de Madrid, Avda. Universidad 30, 28911 Leganés, Madrid, Spain

Abstract

In the interest of reducing the size of absorption chillers, a novel adiabatic membrane-based micro-absorber prototype is experimentally studied. Water–lithium bromide solution is used as the working fluid flowing through 50 rectangular microchannels of 0.15 mm height, 3 mm width and 58 mm length. In the present study, a laminated microporous PTFE membrane of 0.45 μm pore diameter, separating the solution from the vapour, is tested. It incorporates a supporting layer of polypropylene. Different operating parameters were tested, including the inlet solution mass flow rate, temperature and concentration and the pressure potential for absorption. The measured concentration and temperature of the solution at the absorber outlet are used to evaluate the mass transfer characteristics of the micro-absorber. It is demonstrated that the process is controlled by the solution mass transfer resistance. Calculated results of the absorption rate and the absorption ratio show the advantages of the proposed design considering its compactness. The cooling power of a hypothetical chiller equipped with the tested micro-absorber of 73.7 cm^3 effective volume, for the range of variables considered in this study, is 41 W. The modular configuration of the absorber allows to easily scale-up the cooling capacity.

* Corresponding author.
E-mail address: mvenegas@ing.uc3m.es (M. Venegas).

Keywords: Absorption refrigeration; adiabatic micro-absorber; membranes; rectangular microchannels; water–lithium bromide

Nomenclature

A	area (m^2)
AR	absorption ratio (kg_{va} kg_{si}^{-1})
d_p	membrane pore diameter (m)
e	height or thickness (m)
J	absorption rate (kg m^{-2} s^{-1})
l	width (m)
L	total length of channels (m)
$\dot{m}$	mass flow rate (kg s^{-1})
M	molecular weight (kg $kmol^{-1}$)
P	pressure (kPa)
R	mass transfer resistance (kg^{-1} Pa m^2 s)
R_u	universal gas constant
T	temperature (ºC)
x	lithium bromide mass fraction (kg_{LiBr} kg_s^{-1})

Greek symbols

ε	porosity
ρ	density (kg m^{-3})
τ	tortuosity

Subscripts

i	inlet
m	membrane
o	outlet
s	solution
v	vapour
va	vapour absorbed
w	wall

1. Introduction

The use of air-conditioning for space cooling is expected to rapidly increase due not only to the rise in global temperatures, but also because the higher incomes in developing countries and the derived urbanization advances. According to estimations of Isaac and van Vuuren [1], the demand for residential space cooling will rise from close to 300 TWh in 2000 to about 4000 in 2050 and more than 10,000 in 2100. Over the next 30 years, according to the European Comission [2] and Jakubcionis and Carlsson [3], the energy used to cool buildings across Europe is likely to increase from about 35 TWh in 2015 to 78 TWh or even 137 TWh in 2050 (depending on the considered scenario). At present, mechanical compression systems provide most of the space cooling demand, contributing to global warming and greenhouse effect, which could increase accordingly to the cooling demand.

Absorption chillers can effectively help to the reduction of CO_2 emissions as they can use waste heat or renewable heat from solar thermal collectors in the form of hot water for cooling purposes instead of fossil fuels for the electricity production. The conventional configuration of the current systems employs shell and tubes heat and mass exchangers with cooling power to absorber volume ratios around 451 kW/m^3 [4]. These shell and tubes exchangers have been successfully employed for cooling demands in the order of tenths of kW or larger capacities. For lower cooling demands no absorption units are commercially available for using in dwellings air-conditioning appliances.

Recently, the utilization of membrane contactors in absorption cooling chillers has been considered as an alternative technology for minimizing the size of these devices. Because of its novelty, in the open literature, limited investigations have been carried out on the utilization of membrane contactors in absorption cooling chillers. Major part of the papers have been published in the last decade. A review of these systems has been done by Asfand and Bourouis [5].

While previous works using the ammonia-water solution have already remarked the high potential of the membrane absorption technology for volume and cost reduction of absorption refrigerators, we will focus our research in the use of membrane-based absorbers working with the water-lithium bromide (H_2O-LiBr) solution. The chillers using this solution do not require a rectification column, reach higher COPs and are specially recommended for air-conditioning applications.

Schwerdt [6] presented experimental results obtained using the H_2O-LiBr solution. According to Ali and Schwerdt [7,8], the main parameters to take into account in the selection of the membrane, when working with the H_2O-LiBr solution, are: no capillary condensation of water vapour should occur in the membrane to avoid blocking of the pores, the membrane thickness should take into account the resistance to mass transfer, and the mechanical stability. A layer thickness up to 60 microns is a good compromise between both constraints. A large pore diameter combined with a porosity value of 0.8 leads to an almost doubled water vapour flux through the membrane compared to a porosity value of 0.5. The appropriate membrane should have a porosity ranging between 0.7 and 0.8.

Considering the solution film thickness and solution velocity, experimental studies of absorbers using the H_2O-LiBr solution and a hydrophobic membrane of Ali and Schwerdt [7], and simulations of Yu et al. [9] and Asfand et al. [10], lead to the main similar conclusion: the absorption rate increases if the solution film thickness is reduced and the solution velocity increases.

Isfahani and Moghaddam [11] tested an absorber using the H_2O-LiBr solution and a superhydrophobic nanofibrous membrane with nominal pore size of 1 micron and 80% porosity. They obtained an absorption rate of about 0.006 kg/m^{2}s, using channels of 100 micron thickness and a flow velocity of 5 mm/s. Isfahani et al. [12] presented a study on the efficacy of highly porous nanofibrous membranes for application in membrane-based absorbers and generators. Permeability studies showed that membranes with a pore size greater than about 1 micron are valid for application in the absorber, while smaller pores were found to be adequate for the generator. Some improvements to the simple configuration of microchannels are now under investigation in order to increase the absorption rate. Bigham et al. [13] used a combination of experimental and numerical studies to illustrate the absorption/desorption process to/from a solution flow confined within microchannels to study the impact of surface microstructures on the absorption/desorption process, respectively. Isfahani et al. [14] used also surface structures to manipulate the thermohydraulic characteristics of the H_2O-LiBr solution flow in a membrane-based absorber.

Venegas et al. [15] developed a simple model of a miniaturized absorber using membrane technology validated using data of Isfahani and Moghaddam [11]. With this model a parametric study evaluated the sensitivity of the ratio between the cooling capacity of the chiller and the water-cooled absorber volume to changes in some

operating and design parameters (Venegas et al. [16]). It was concluded that, at the design stage, the most important parameters are porosity, pore diameter, solution channels depth and membrane thickness. For an optimal performance during the operation of the absorber, special care should be taken to select the adequate vapour pressure and solution inlet temperature and concentration.

All of the previous studies considered the extraction of the absorption heat by a cooling water flow. Besides, a further reduction in size of the absorber could be achieved using adiabatic membrane microchannel heat exchangers. The processes related to the mass and heat transfer in adiabatic absorbers was considered by Venegas et al. [17], where a comparison between the adiabatic and the non-adiabatic membrane-based absorbers using the water-lithium bromide solution served to identify the least volume configuration. The final objective of the comparison was to minimize the absorber volume, in order to reduce the size of absorption cooling chillers. The adiabatic configuration has significant advantages respect to the non-adiabatic one in terms of higher cooling power to absorber volume ratios and fabrication simplicity.

As can be seen from the literature review, there are no papers related to the experimental evaluation of an adiabatic microchannel membrane-based absorber. Therefore, a specific module has been built and tested. The present paper presents the analysis of an adiabatic absorber using rectangular microchannels and a microporous membrane. The module contains a vapour channel, separated from the solution by an adjacent microporous membrane. The solution is confined in the rectangular microchannels. A metallic wall separates the solution channels between them. Results obtained for different solution mass flow rates, temperatures, driving pressures and solution concentrations allow the evaluation of the mass transfer process in this kind of novel adiabatic micro-absorber.

2. Experimental setup

A schematic cross-section and a photograph of the micro-absorber used in the current study are shown in Fig. 1. It is a plate-and-frame membrane module, with the geometrical data described in Table 1. The module contains a vapour channel, separated from the solution by an adjacent microporous membrane. The solution flows confined in rectangular microchannels mechanized in an AISI 316L plate (Fig. 2). Cooling water

channels are avoided because an adiabatic configuration is used. Additionally, a thin perforated plate (Fig. 3) is located over the membrane, to keep it attached to the channel walls.

a)

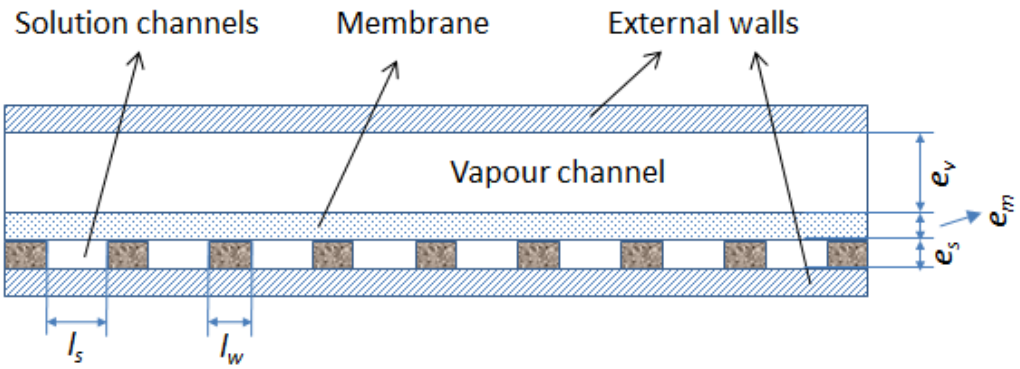

b)

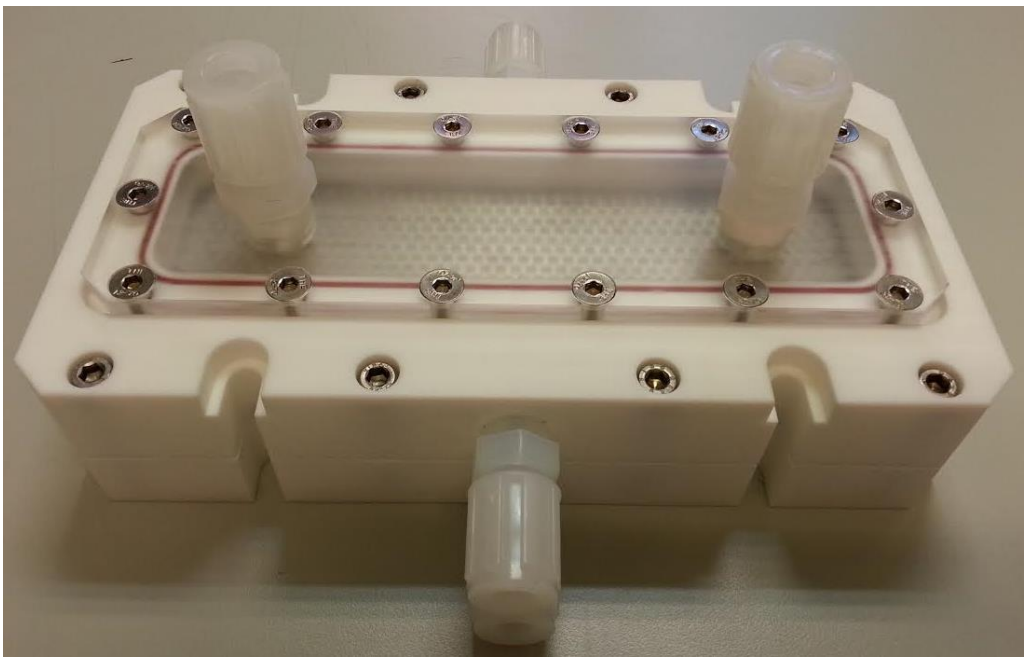

Fig. 1. a) Cross-sectional scheme of the adiabatic absorber. b) Absorber tested.

Table 1. Geometrical data of the absorber, corresponding to the scheme represented in Fig. 1.

Parameter	Value
Vapour channel height, e_v (mm)	5
Solution channel height, e_s (mm)	0.15
Solution channel width, l_s (mm)	3
Width of the intermediate wall between channels, l_w (mm)	0.75
Length of channels, L (cm)	5.8

Fig. 2. Stainless steel plate incorporating the rectangular microchannels.

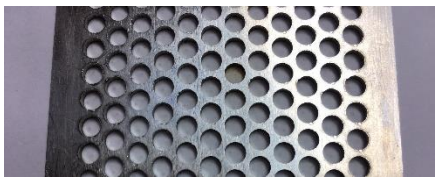

Fig. 3. Photograph of the stainless steel supporting plate, 1.5 mm thick, with holes of 3.2 mm diameter.

The membrane characteristics correspond to a commercially available membrane, usable in absorbers with the H_2O-LiBr solution. The membrane selected, PTFE0453005 of Sterlitech [18], is shown in Fig. 4. Its main characteristics, detailed in Table 2, include thickness, porosity and pore diameter data.

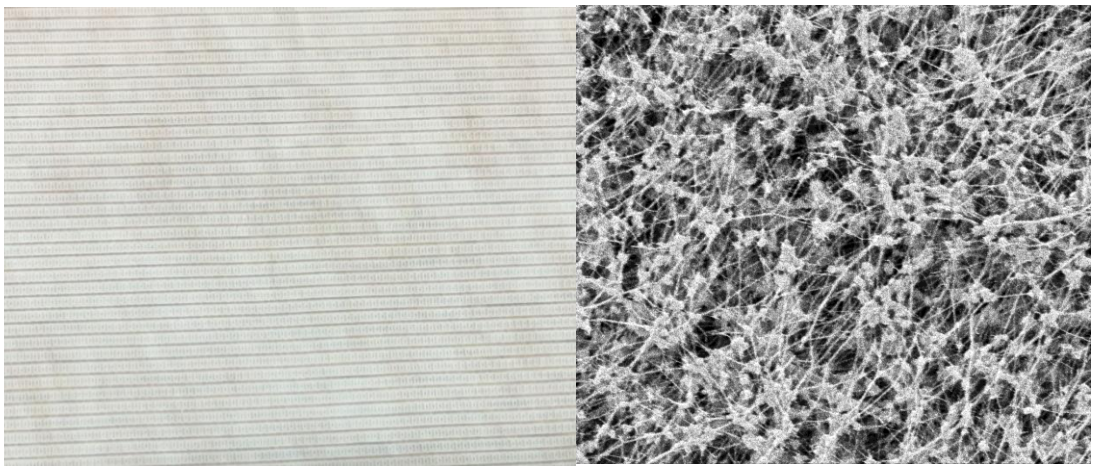

Fig. 4. Membrane used in the experimental tests (PTFE0453005). Microscopic image taken from Sterlitech [18].

Table 2. Data of the membrane tested.

Parameter	PTFE0453005
Supporting layer of polypropylene	Yes
Thickness, e_m (μm)	76-127
Porosity (%)	~90
Pore diameter, d_p (μm)	0.45

The absorber is integrated in a test bench for component characterization. The schematic diagram is shown in Fig. 5. It is composed by a vapour generation system and a solution line, including two solution tanks, a circulation pump and the absorber. The measurement system incorporates two flowmeters, 5 pressure transducers and 6 thermoresistances. Stainless steel construction and inert polymers ensure a long life against corrosion. Two Coriolis type flowmeters (CFMS010M), manufactured by Micromotion™, allow measuring the mass flow rate and density of the concentrated and diluted solution. The solution pump is of magnetic type and its flow rate is controlled by a variable frequency driver. Temperature sensors, thermoresistance PT100 (OMEGA series PR-17), and absolute pressure transducers (OMEGA PX409-005AI-EH) are used at the inlet and outlet of the absorber. Uncertainty data of the measured variables are specified in Table 3. They correspond to the values provided by the manufacturer of each sensor. A photograph of the complete experimental test bench is shown in Fig. 6.

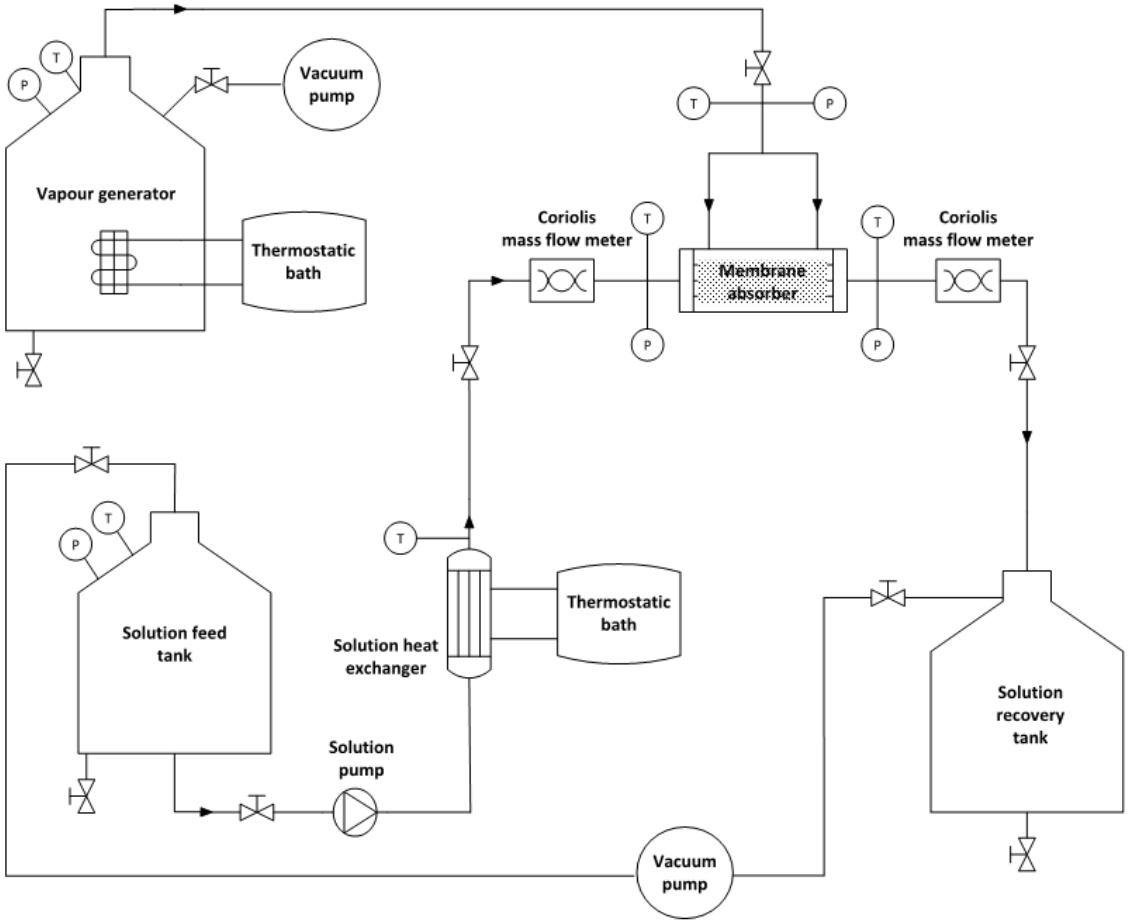

Fig. 5. Scheme of the test bench.

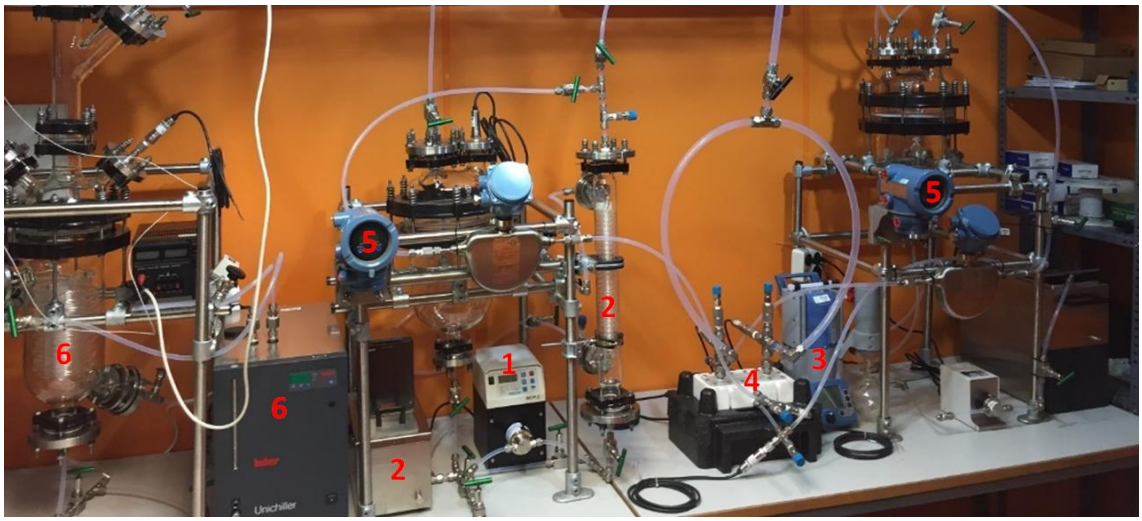

Fig. 6. Photograph of the test bench. 1-solution pump, 2-thermostatic system for temperature regulation, 3-vacuum pump, 4-absorber, 5-Coriolis flowmeters, 6-vapour generation system.

Table 3. Uncertainty of measured variables.

Variable	Type of sensor	Range	Uncertainty
T	Platinum PT100 class A	-30 – 350 ºC	± (0.15+0.002*T) ºC
ρ	Coriolis flowmeter	0 – 5000 kg/m^3	± 0.5 kg/m^3
P	Absolute pressure transducer	0 – 5 psi	± 0.05% f.s.
$\dot{m}$	Coriolis flowmeter	0.002 – 110 kg/h	± 0.1%

The facility incorporates a data acquisition system controlled by a computer. Data acquired by all of the flowmeters and by the temperature and pressure transducers are saved on-line in the computer at intervals of 1 second.

3. Data reduction

The following parameters described in this section are presented in order to completely characterise the mass transfer process in the membrane-based absorber.

3.1. Absorption ratio

The vapour mass flow rate through the membrane ($\dot{m}_{va}$) is calculated taking into account the conditions of the outlet and inlet streams in the absorber:

$$\dot{m}_{va} = \dot{m}_{so} - \dot{m}_{si} \quad (1)$$

The absorption ratio AR indicates how much vapour is being absorbed by each kilogram of solution circulated (Warnakulasuriya and Worek [19], Acosta-Iborra et al. [20]). It is useful for cycle evaluation, as it is the inverse of the circulation ratio for single pass absorbers:

$$AR = {\dot{m}_{va}}/{\dot{m}_{si}} \quad (2)$$

3.2. Absorption rate

The absorption rate (J) depends on the mass flow rate of vapour absorbed and the mass transfer area (A):

$$J = {\dot{m}_{va}}/{A} \quad (3)$$

The area A is calculated considering the effective contact area between the membrane and the vapour channel. In this case it corresponds to that of the circular

holes of 3.2 mm diameter, manufactured in the supporting stainless steel plate shown in Fig. 3, which fixes the membrane to the top of the solution channels.

3.3. Mass transfer resistance

The overall mass transfer resistance is calculated using Eq. (4):

$$R = \frac{P_v - P_s}{J} \tag{4}$$

P_v and P_s in Eq. (4) are, respectively, the pressure in the vapour channel and the partial pressure of the water vapour, calculated at the inlet solution temperature (T_{si}) and concentration (x_i). The overall mass transfer resistance between water vapour and solution (R) includes the resistance to diffusion through the solution boundary layer (R_s) and the resistance to diffusion of water vapour through the membrane (R_m).

Depending on the value of the ratio between the molecules mean free path and the pore diameter (Knudsen number), different mechanisms for vapour transport through the membrane exist: Knudsen diffusion, transition flow and viscous flux (Poiseuille flow). For each of these regimes, the transport resistance R_m is calculated in different ways. For the experimental conditions used in the present work, Knudsen number varies from 6.2 to 8.9. Consequently, a transition flow occurs through the membrane in the absorber. In this case, according to the resistance analogy, the mass transport resistance can be written as:

$$\frac{1}{R_m} = \frac{M}{e_m}\left(\frac{D_e^K}{R_u T_m} + \frac{P_m B_0}{R_u T_m \mu_v}\right) \tag{5}$$

where:

$$D_e^K = \frac{\varepsilon d_p}{3\tau}\left(\frac{8 R_u T_m}{\pi M}\right)^{0.5} \tag{6}$$

$$B_0 = \frac{\varepsilon d_p^2}{32\tau} \tag{7}$$

In Eqs. (5) and (6), M is the molecular weight of water and R_u is the universal gas constant. In Eqs. (6) and (7), ε and τ are the porosity and tortuosity of the membrane, respectively. Tortuosity is calculated as a function of the membrane porosity, according to Iversen et al. [21]:

$$\tau = \frac{(2-\varepsilon)^2}{\varepsilon} \tag{8}$$

Finally, the solution mass transfer resistance is calculated from:

$$R_s = R - R_m \tag{9}$$

Thermodynamic properties of the water-lithium bromide solution and water are calculated using correlations developed by Patek and Klomfar [22] and Harr et al. [23].

The viscosity and thermal conductivity of the water-lithium bromide solution are computed using correlations provided by Lee et al. [24] and DiGuilio et al. [25]. The transport properties of water are calculated using equations of the Electrical Research Association [26].

4. Results and discussion

In the present study, experiments were conducted for evaluating the mass transfer in the adiabatic micro-absorber. Some operating parameters controlling the process were modified, including the inlet solution concentration, temperature and mass flow rate and the pressure potential. The influence of these variables on the outlet solution concentration and temperature, mass transfer resistances, absorption ratio and absorption rate is shown in the following. An estimation of the cooling power that could be provided with the adiabatic micro-absorber when used in a complete chiller is presented.

Table 4 gives the average and maximum uncertainties obtained for the main variables calculated in the present work (Taylor and Kuyatt [27]).Very low uncertainties are shown, due to the high accuracy of the instrumentation used.

Table 4. Results of the uncertainty analysis for calculated variables.

Variable	Average	Maximum
Outlet solution concentration, x_o	0.05%	0.05%
Pressure potential, P_v - P_s	0.5%	0.6%
Absorption ratio, AR	1.8%	3.8%
Overall mass transfer resistance, R	1.8%	3.9%
Membrane mass transfer resistance, R_m	0.02%	0.02%
Solution mass transfer resistance, R_s	2.1%	4.2%
Absorption rate, J	1.8%	3.8%
Cooling power, Q	1.8%	3.8%

Experimental results shown in Figs. 7 to 11 were conducted at an inlet concentration of 58.6%, with a standard deviation of 0.07%. The inlet solution temperature in these experiments was 27.3 ºC, with a standard deviation of 0.007 ºC. Temperature of the vapour generated in the thermostatic bath ranged between 31 and 34.7 ºC. This

temperature does not influence the vapour absorption process, as shown in Venegas et al. [16]. Only the vapour pressure, fixing the pressure potential for mass transfer, governs the process.

Fig. 7 shows the evolution of the solution concentration and density at the inlet and outlet of the adiabatic absorber as a function of the pressure potential. This pressure potential is defined as the difference between the vapour pressure and the partial pressure of the water vapour, calculated at the inlet solution temperature and concentration. Inlet and outlet densities were measured using the Coriolis flowmeters, while the concentrations were calculated using the correlation of Patek and Klomfar [22] as a function of the measured density and temperature. A linear relationship is observed in Fig. 7 between the solution concentration and the pressure potential. An increase of the latter produces a higher mass transfer from the vapour channel to the solution side, diluting more the solution. For example, when the pressure potential increases from 3.1 to 3.8 kPa, the solution concentration change rises from 1.4% to 3.5%. This pressure potential corresponds, for example, to the case of using hybrid absorption-compression cooling systems, in which a vapour compressor is used at the evaporator outlet, as shown in Schweigler et al. [28]. These hybrid systems allow increasing the COP of the cycle.

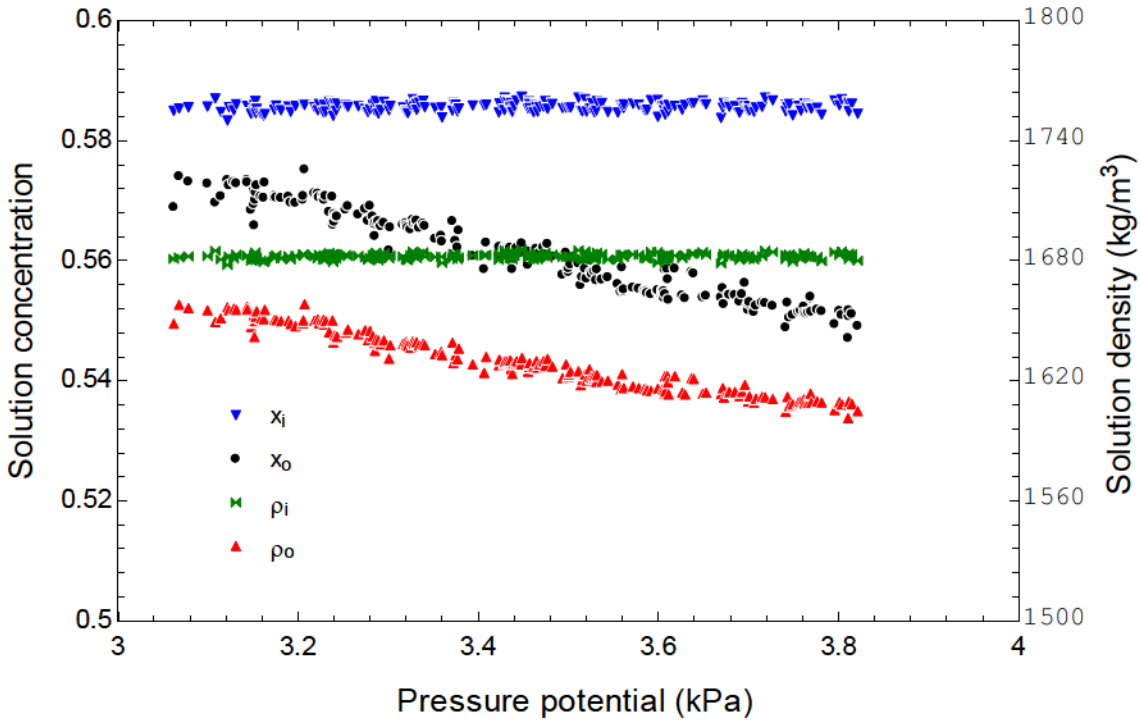

Fig. 7. Solution concentration and density at the inlet and outlet of the absorber as a function of the pressure potential.

Inlet and outlet measured solution temperatures in the adiabatic absorber are shown in Fig. 8 as a function of the pressure potential. The outlet temperature increases with the pressure potential. This is a result of the increase in water vapour absorption (as shown in Fig. 7), which releases more heat in the process. This heat is stored in the solution because no external cooling water flow is used in the configuration tested, contributing to the increase of the solution temperature. The very high outlet temperature values obtained in the current study show the possibilities of the adiabatic absorber to increase the performance of the absorption cycle, due to the preheating effect of the solution flowing to the desorber. In the conditions tested, temperatures of up to 52 ºC are obtained at the absorber outlet. As a result, the dimensions of the heat recoverer can be reduced or evenly eliminated. In order to improve the total amount of vapour absorbed, the solution can be subcooled in an external heat exchanger and recirculated through the absorber.

The saturation temperature, calculated at the average solution pressure and concentration between the inlet and outlet of the absorber, is also represented in Fig. 8. It represents the temperature that the solution would reach in the case of becoming saturated (equilibrium condition). It can be observed that the outlet temperature is still below the saturation value even at the highest pressure potential used in the tests. It means that the absorber length or the pressure potential can still be increased to reach saturation.

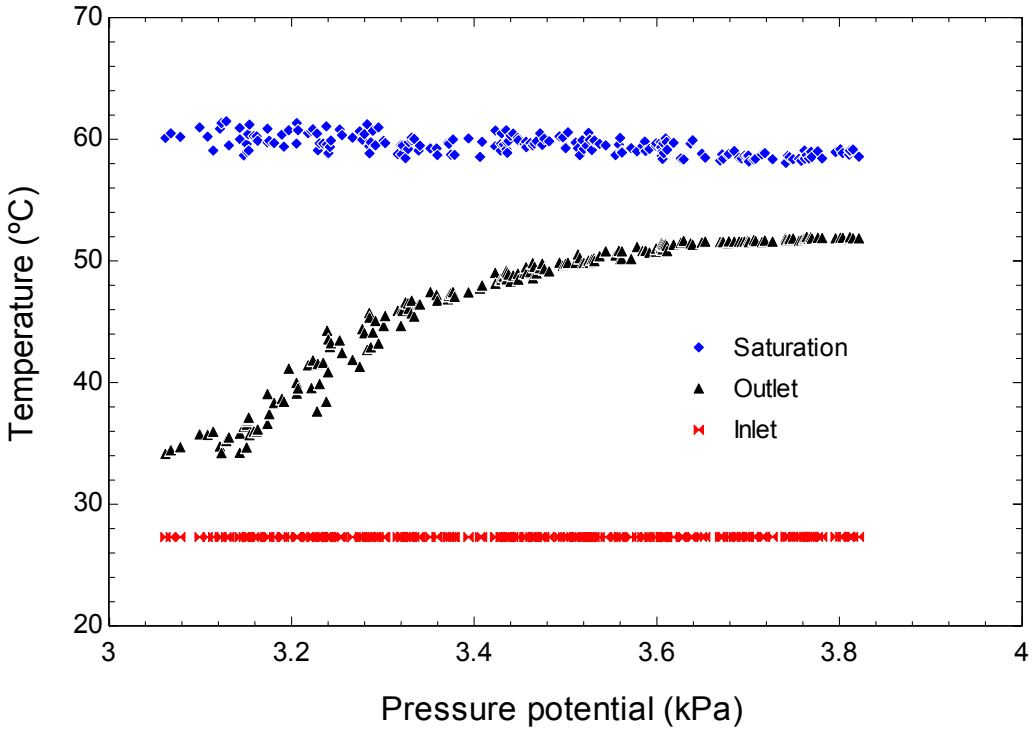

Fig. 8. Solution temperature at the inlet and outlet of the absorber and saturation temperature as a function of the pressure potential.

The different overall, membrane and solution mass transfer resistances were calculated as described in section 3. They are represented in Fig. 9 as a function of the pressure potential. In the present study the membrane resistance is much lower than the solution resistance. It represents between 6.9% and 24.8% of the overall mass transfer resistance. This result is similar to data reported by Isfahani and Moghaddam [11]. In their experimental study the membrane resistance represented only between 10 and 15% of the total resistance. According to these results, the solution resistance is the most limiting and should be reduced in order to improve the mass transfer process. One way to improve the solution mass transfer coefficient is to increase the solution velocity. In the present study the velocity in the channels ranged from 3.8 mm/s to 7.7 mm/s.

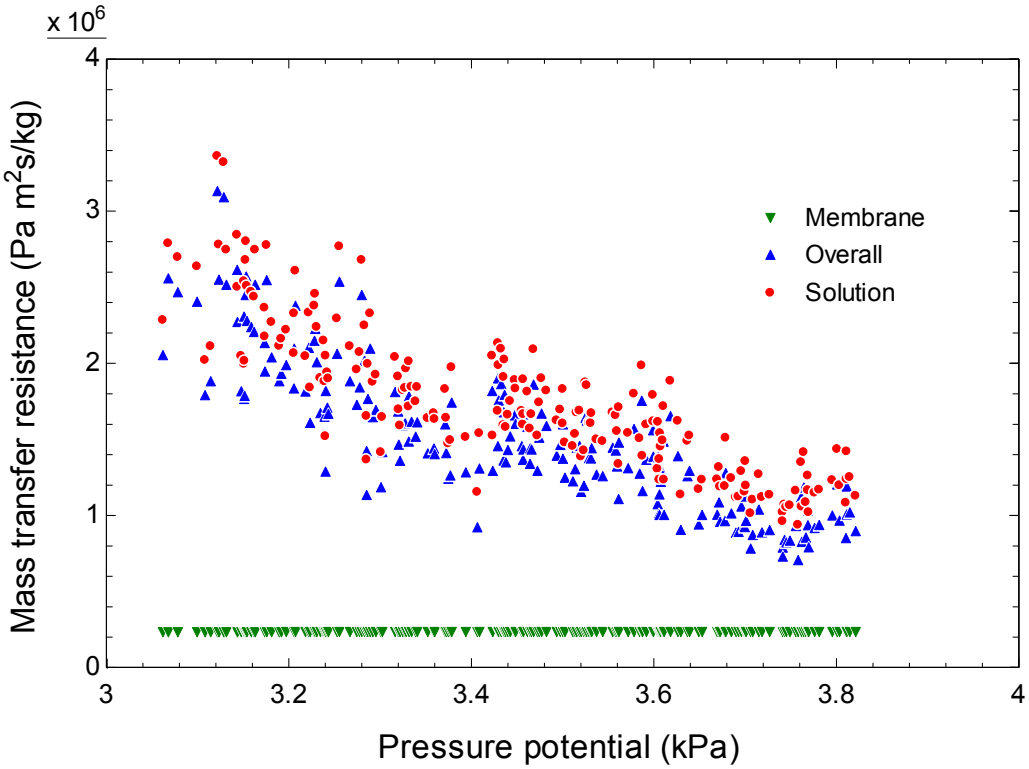

Fig. 9. Membrane, solution and overall mass transfer resistance as a function of the pressure potential.

The absorption ratio obtained in the experiments is shown in Fig. 10 as a function of the pressure potential. A positive linear relation is observed between both parameters, indicating that the absorption capacity is directly related to the pressure potential. Current absorption ratios (from 0.017 to 0.071 kg_{va}/kg_{si}) are higher than those obtained in previous works performed using other configurations of adiabatic absorbers based on water as refrigerant. Palacios et al. [29], using H_2O-LiBr, obtained ratios below 0.016 kg_{va}/kg_{si}, while Warnakulasuriya and Worek [19], using H_2O-LZB^{TM}, reached 0.0055 kg_{va}/kg_{si} as maximum. These last research were performed using adiabatic chambers in which the solution was injected using various types of atomizers, dispersing the solution in drops or sheets. Reasons for the differences may be attributed mainly to changes in the configuration of the absorber, from cylindrical chambers to membrane-based microchannels, and the operating conditions used during experiments.

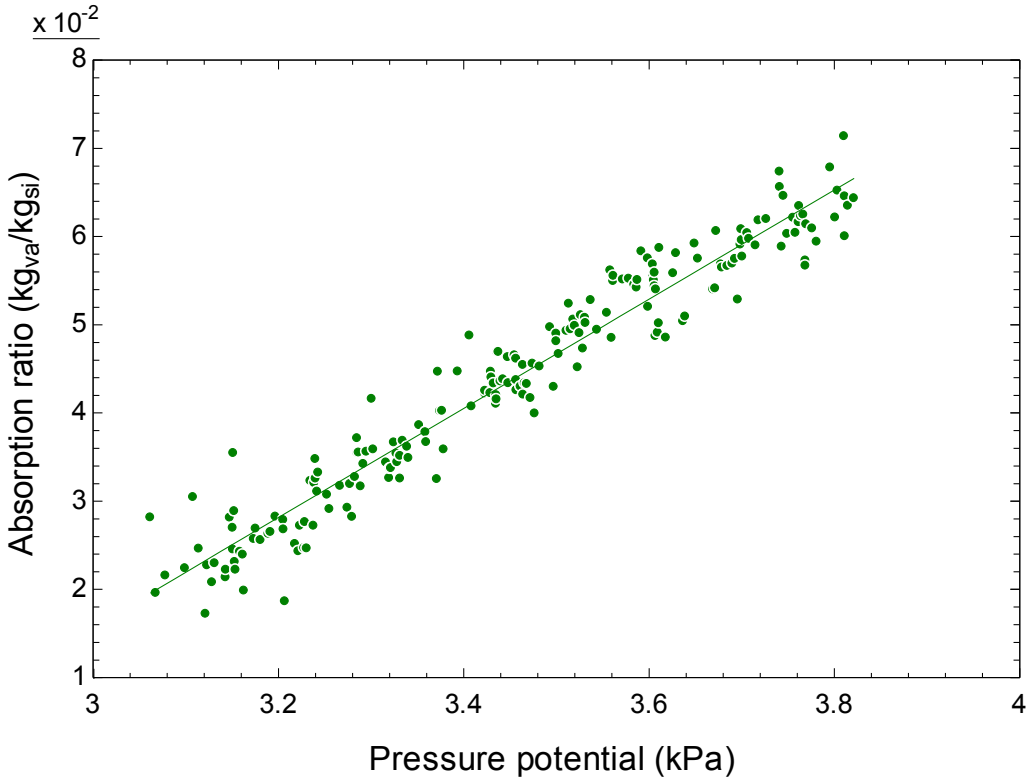

Fig. 10. Absorption ratio as a function of the pressure potential.

Fig. 11 shows, in the left axis, the absorption rate as a function of the solution mass flow rate, for different values of the pressure potential. As expected, an increase of the flow rate augments the amount of solution in contact with the vapour per second, increasing the mass transfer. A larger pressure potential also contributes to improve the absorption process, as discussed previously. The range of absorption rates obtained in the present work are lower than those reported by Isfahani and Moghaddam [11] and Isfahani et al. [12]. In their studies, absorption rates in the order of $1.7 \cdot 10^{-3}$ to $7.8 \cdot 10^{-3}$ kg/m^{2}s were obtained. Main cause for this difference is related to the adiabatic process taking place in the current study, while cooling water was used in the cited research to extract the heat released during absorption. The adiabatic absorption process increases the temperature of the solution, reducing the potential for mass transfer respect to a non-adiabatic process. Further reasons for the differences between current and previous results are associated to dissimilar operating conditions, including different pressure potential, and geometrical parameters used. These include different channel dimensions (height, width and length), mass flow rates, solution and vapour pressures, solution inlet temperature and concentration and membrane type. Results of Isfahani and Moghaddam [11] are cited now because it is the only experimental research found in the open

literature using a membrane-based absorber with rectangular microchannels and the same solution.

On the right side of Fig. 11 the estimated cooling power of a hypothetical chiller equipped with the novel tested micro-absorber is shown. The cooling capacity is calculated through $q_e = \dot{m}_{vd} h_{fg}$. The vaporization enthalpy, h_{fg}, is obtained considering that the evaporator is working at the pressure in the solution channels. For the conditions essayed this cooling power reaches a maximum of 41 W. The effective volume of the micro-absorber, taking into account the dimensions of the solution and vapour channels, the membrane and the supporting plate, is 73.7 cm^3. The maximum ratio between the cooling power and the absorber volume obtained is 559 kW/m^3. The high value of the cooling power density is associated to the high vapour pressure (pressure potential) used in the experiments. This value is higher than the ones obtained using falling film absorbers of conventional-diameter tubes [4].

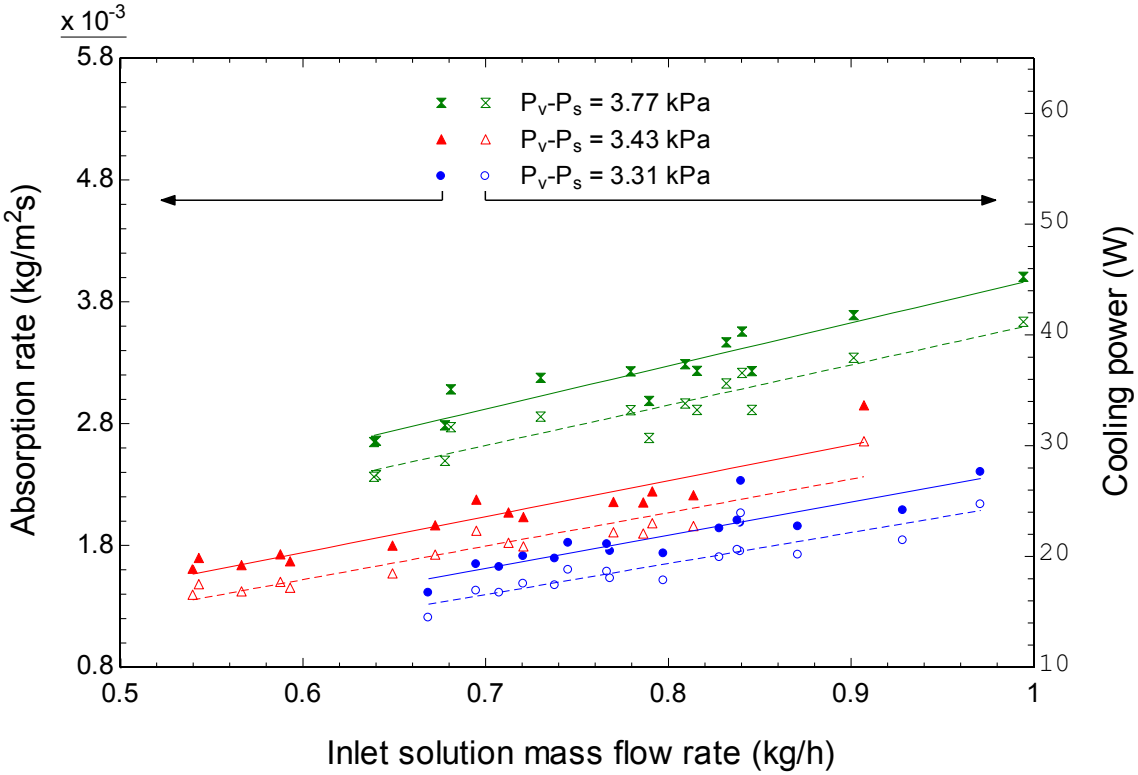

Fig. 11. Absorption rate and cooling power as a function of the inlet solution mass flow rate for different pressure potentials. Continuous and dash lines corresponds to the linear fit of the absorption rate and the cooling power data points, respectively.

The pressure drop along the channels was estimated using correlation of Kandlikar et al. [30]. It varies between 0.8 and 1.5 kPa. Pressure drop is an important parameter in the performance of the chiller. A pressure reduction translates in a decrease of the saturation temperature for the given solution mass fraction. Consequently, in the case of the absorber, this saturation temperature decrease reduces the amount of water vapour able to be absorbed.

As it has been shown in previous results, the pressure potential has a strong influence on the mass transfer process. The effect of the inlet solution concentration and temperature is included inside this pressure potential, because the partial pressure of the water vapour (P_s) is calculated on the base of these variables. Fig. 12 shows two different cases, one corresponds to a colder and diluted solution (T_{si} = 25.3 ºC, x_i = 51.2%) and the other one to a less cold and concentrated solution (T_{si} = 27.3 ºC, x_i = 58.6%). However, both cases have the same pressure potential, equal to 3.4 kPa. As it can be observed, the effect of the mass flow rate on the absorption rate is similar in both set of experiments. For the new temperature and concentration, the numerical values of the absorption rate are lower, in correspondence with the lower solution mass flow rate, which contributes to reduce the amount of vapour absorbed.

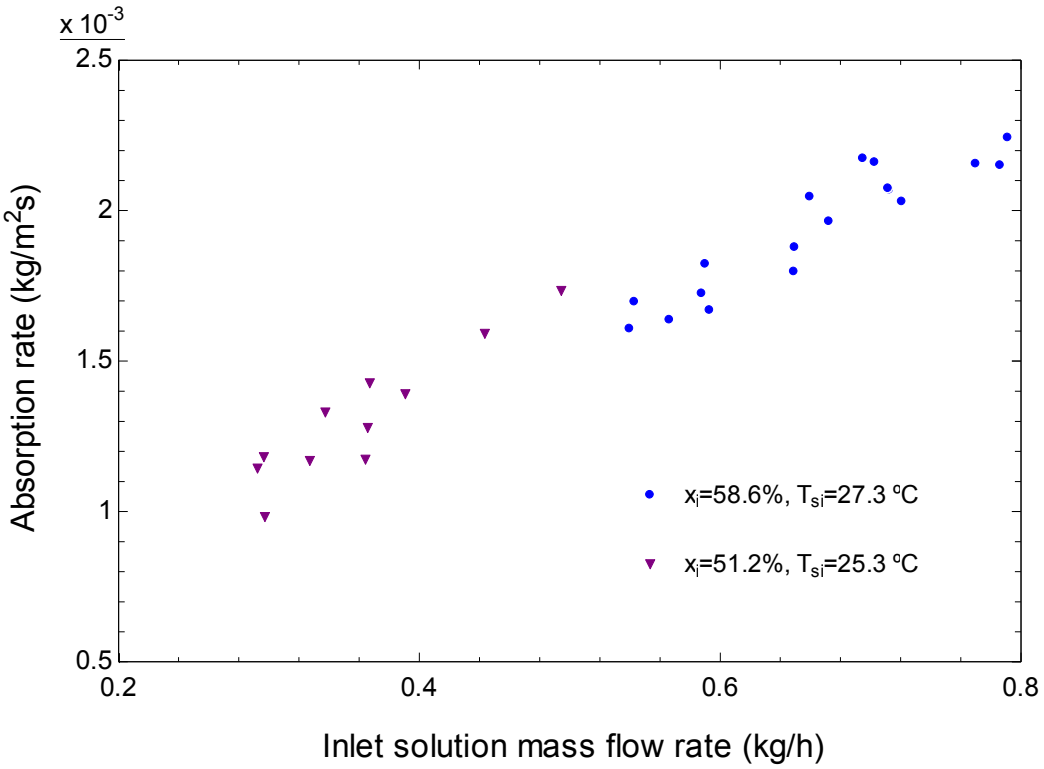

Fig. 12. Absorption rate as a function of the inlet solution mass flow rate. P_v-P_s = 3.4 kPa.

5. Conclusions

In this work an adiabatic membrane-based microchannel absorber has been experimentally evaluated using the water-lithium bromide solution. A laminated microporous PTFE membrane has been used in combination with rectangular microchannels. The following conclusions have been derived from the experimental study:

- As absorption proceeds along the channels the heat released is stored in the solution increasing its temperature. At the absorber outlet the solution temperature is lower than the saturation value, indicating that the solution still has capacity for further absorption. A higher pressure potential approaches the outlet solution temperature to the equilibrium condition.
- The solution mass transfer resistance is dominant in the absorption process. It represents between 85.6 and 96% of the overall resistance. It means that the membrane resistance is unimportant for the essayed conditions and efforts should be devoted to improve the solution mass transfer coefficient.
- Absorption ratios obtained are higher than those reported in previous works using water-based solutions in adiabatic absorption chambers. The present design is advantageous because it allows improved absorption ratios in a more compact configuration.
- In the same way to other studies in non-adiabatic membrane-based absorbers, a positive linear relation has been obtained between the absorption rate and the solution mass flow rate. In a similar way, an increase in the pressure potential improves the absorption rate.
- Absorption rates obtained in the present work are lower than those reported in water-cooled membrane-based absorbers. In order to improve the total amount of vapour absorbed, the solution can be externally cooled and recirculated. Main advantages of the adiabatic configuration here proposed are the reduction in absorber size and the preheating effect obtained for the solution, which reduces the amount of heat to be supplied in the generator. More compact adiabatic absorbers can be obtained using a parallel configuration, in which the vapour channel is shared by two opposed solution channels, and thinner supporting plates.

Acknowledgements

The financial support of this study by the Ministerio de Economía, Industria y Competitividad of Spain through the research grant DPI2017-83123-R is greatly appreciated.

References

[1] M. Isaac, D.P. van Vuuren, Modeling global residential sector energy demand for heating and air conditioning in the context of climate change, Energy Policy 37 (2009) 507–521.

[2] European Commission, Commission staff working document on an EU Strategy for Heating and Cooling, SWD(2016) 24 final, Part 2/2, 2016.

[3] M. Jakubcionis, J. Carlsson, Estimation of European Union residential sector space cooling potential, Energy Policy 101 (2017) 225–235.

[4] S. Jeong, S. Garimella, Optimal design of compact horizontal tube LiBr/water absorbers, HVAC&R Res. 11 (2005) 27–44.

[5] F. Asfand, M. Bourouis, A review of membrane contactors applied in absorption refrigeration systems, Renew. Sust. Energ. Rev. 45 (2015) 173–191.

[6] P. Schwerdt, Activities in thermal driven cooling at Fraunhofer Umsicht. In: Thermally driven heat pumps for heating and cooling. Ed. Annett Kühn. Universitätsverlag der TU Berlin (2013) 117–126.

[7] A.H.H. Ali, P. Schwerdt, Characteristics of the membrane utilized in a compact absorber for lithium bromide-water absorption chillers, Int. J. Refrig. 32 (2009) 1886–1896.

[8] A.H.H. Ali, P. Schwerdt, For designing a compact absorber with membrane contactor at liquid-vapor interface: influence of membrane properties on water vapour transfer, ASHRAE Trans. 116 (2010) 398–407.

[9] D. Yu, J. Chung, S. Moghaddam, Parametric study of water vapour absorption into a constrained thin film of lithium bromide solution, Int. J. Heat Mass Transf. 55 (2012) 5687–5695.

[10] F. Asfand, Y. Stiriba, M. Bourouis, CFD simulation to investigate heat and mass transfer processes in a membrane-based absorber for water-LiBr absorption cooling systems, Energy 91 (2015) 517–530.

[11] R.N. Isfahani, S. Moghaddam, Absorption characteristics of lithium bromide (LiBr) solution constrained by superhydrophobic nanofibrous structures, Int. J. Heat Mass Transf. 63 (2013) 82–90.

[12] R.N. Isfahani, K. Sampath, S. Moghaddam, Nanofibrous membrane-based absorption refrigeration system, Int. J. Refrig. 36 (2013) 2297–2307.

[13] S. Bigham, D. Yu, D. Chugh, S. Moghaddam, Moving beyond the limits of mass transport in liquid absorbent microfilms through the implementation of surface-induced vortices, Energy 65 (2014) 621–630.

[14] R.N. Isfahani, S. Bigham, M. Mortazavi, X. Wei, S. Moghaddam, Impact of micromixing on performance of a membrane-based absorber, Energy 90 (2015) 997–1004.

[15] M. Venegas, M. de Vega, N. García-Hernando, U. Ruiz-Rivas, A simple model to predict the performance of H_2O-LiBr absorber operating with a microporous membrane, Energy 96 (2016) 383–393.

[16] M. Venegas, M. de Vega, N. García-Hernando, Parametric study of operating and design variables on the performance of a membrane-based absorber, Appl. Therm. Eng. 98 (2016) 409–419.

[17] M. Venegas, M. de Vega, N. García-Hernando, U. Ruiz-Rivas, Adiabatic vs non-adiabatic membrane-based rectangular micro-absorbers for H_2O-LiBr absorption chillers, Energy 134 (2017) 757–766.

[18] https://www.sterlitech.com/catalog/product/view/id/2651/s/ptfe-laminated-membrane-filter-ptfe0453005/. Last accessed 27 June 2018.

[19] F.S.K. Warnakulasuriya, W.M. Worek, Adiabatic water absorption properties of an aqueous absorbent at very low pressures in a spray absorber, Int. J. Heat Mass Transf. 49 (2006) 1592–1602.

[20] A. Acosta-Iborra, N. García, D. Santana, Modelling non-isothermal absorption of vapour into expanding liquid sheets, Int. J. Heat Mass Transf. 52 (2009) 3042–3054.

[21] S.B. Iversen, V.K. Bhatia, K. Dam-Johansen, G. Jonsson, Characterization of microporous membranes for use in membrane contactors, J. Membr. Sci. 130 (1997) 205–217.

[22] J. Patek, J. Klomfar, A computationally effective formulation of the thermodynamic properties of LiBr-H2O from 273 to 500 K over full composition range, Int. J. Refrig. 29 (2006) 566–578.

[23] L. Harr, J.S. Gallagher, G.S. Kell, NBS/NRC steam tables. Hemisphere Publishing Co., New York, 1984.

[24] R.J. Lee, R.M. DiGuilio, S.M. Jeter, A.S. Teja, Properties of lithium bromide-water solutions at high temperatures and concentrations - II density and viscosity, ASHRAE Trans. RP-527 (1990) 709–714.

[25] R.M. DiGuilio, R.J. Lee, S.M. Jeter, A.S. Teja, Properties of lithium bromide-water solutions at high temperatures and concentrations - I thermal conductivity, ASHRAE Trans. RP-527 (1990) 702–708.

[26] Electrical Research Association Steam Tables, Thermodynamic properties of water and steam; viscosity of water and steam, thermal conductivity of water and steam, Edward Arnold Publishers, London, 1967.

[27] B.N. Taylor, C.E. Kuyatt, Guidelines for evaluating and expressing the uncertainty of NIST measurement results, National Institute of Standards and Technology, NIST technical note 1297, 1994.

[28] C. Schweigler, M. Helm, T. Eckert, Flexible heat pump or chiller with hybrid water/LiBr absorption/compression cycle, Int. J. Refrig. (2018), doi: 10.1016/j.ijrefrig.2018.03.003.

[29] E. Palacios, M. Izquierdo, J.D. Marcos, R. Lizarte, Evaluation of mass absorption in LiBr flat-fan sheets, Appl. Energy 86 (2009) 2574–2582.

[30] S.G. Kandlikar, S. Garimella, D. Li, S. Colin, M.R. King, Single-phase liquid flow in minichannels and microchannels. Elsevier Science, Chapter 3, 2006.